

# UWB On-body Slotted Patch Antennas for In-Body Communications

Enrique Miralles<sup>1</sup>, Carlos Andreu<sup>1</sup>, Marta Cabedo-Fabrés<sup>1</sup>, Miguel Ferrando-Bataller<sup>1</sup>, Jose F. Monserrat<sup>1</sup>

<sup>1</sup> Institute of Telecommunications and Multimedia Applications, Universitat Politècnica de València, Valencia, Spain,

\* *enmigma@teleco.upv.es*

**Abstract**— One of the most relevant challenges of next generation in-body devices consists in enhancing the medical applications of wireless networks qualitatively. The current standard does not allow high data rate wireless connections between implanted nodes. UWB systems have been considered as a potential candidate for future in-body devices. To establish a proper link within UWB, antenna matching should be ensured within the frequency range of interest. Besides, a good wave penetration through the biological tissues is totally essential. In this work, several UWB on-body slotted patch antenna models are assessed and discussed. According to the propagation medium, the on-body antenna designs have been miniaturized and optimized taking into account the dielectric properties of human tissues. After a thorough comparison between antenna models, an optimized model has been manufactured. Finally, the performance of the optimized antenna prototype has been assessed.

**Index Terms**— UWB systems, on-body antennas, in-body communications.

## I. INTRODUCTION

Nowadays, body area networks (BAN) allow wireless connections between implanted nodes. Establishing a feasible link between a capsule endoscope and an on-body sensor array is an instance of the current medical systems. IEEE 802.15.6 is the current standard for this kind of communications. Medical Implant Communication Service (MICS) frequency band, which covers from 402 to 405 MHz, is the standardized frequency range in order to communicate in-body devices. However, MICS systems are constrained in terms of bandwidth (300 kHz). Thus, current in-body devices are not able to get high data rate wireless connections, which are common in other telecommunication services. Therefore, future generation devices aim at enhancing the healthcare and the wellbeing qualitatively. Thorough research works are totally essential in order to improve the current standard for implant communications. In the last decades, Ultra Wide Band (UWB) frequency band (3.1-10.6 GHz) has emerged as a potential candidate for in-body connections [1]. This is due to its main benefits such as large bandwidth, low profile of its devices, low power consumption and so on. However, the attenuation through the biological tissues increases dramatically as the frequency increases [2]. Thereby, many research works consider the low part of UWB frequency band as the best candidate for the revision of the current standard [3].

In order to perform reliable research studies within UWB, the antennas play a crucial role. Since the propagation medium is not the free space, new antenna designs should consider the dielectric features of human body tissues. In order to establish a proper link between a device implanted within the small intestine and an antenna located over the human body surface, the radio waves go through a non-homogeneous medium. Accordingly, several simulation setups to reproduce the propagation medium in the design stage can be found in the available literature. On the one hand, human voxel models can be used [4]. However, this solution implies a high complex computational cost as well as the use of expensive high performance computer. On the other hand, multilayer models could be a cost-effective solution. In this case, the propagation medium is reproduced by means of different homogeneous human tissue layers [5].

According to the locations of transmitters and receivers, different communication scenarios can be considered. Regarding the in-body to on-body scenario, the implanted antenna is located inside the human body whereas the on-body antenna is placed over the human body surface. With regard to the on-body antenna, a compact structure to be embedded in a belt around the patient's waist is necessary. Besides, the antenna matching should be ensured within the whole frequency band of interest. Moreover, the radio waves within this frequency band should have relatively fair propagation conditions through the human tissues.

In the literature, a high number of UWB on-body antenna designs for on-body to on-body and on-body to off-body communications can be found [6]–[8]. However, the literature is lack of UWB on-body antennas for in-body communications. Slotted patch antennas can achieve large bandwidths with low-profile structures within UWB [9][10]. Hence, this type of antennas might be a reliable candidate for this purpose.

In this work, several UWB on-body slot patch antenna models have been assessed. These antenna models have been designed and optimized by considering the most relevant human tissues of the abdominal region as proposed in [11]. In the design stage, a multilayer model has been considered for mimicking the propagation medium [5]. A reflector plane has been included at the back side of the antenna structure to ensure unidirectional radiation. In this manner, an antenna matching within the low part of UWB frequency range, as well as a high directivity radiation pattern, are ensured, taking into account the heterogeneous medium. After

evaluating some slotted patch structures, an optimized antenna model has been obtained and manufactured.

The paper is organized as follows. In section II, the simulation setups as well as the candidate antenna models are provided. Section III details the antenna performance in both simulation and real setups. Finally, in section IV, the most relevant conclusions are summarized.

## II. ANTENNA DESIGNING

### A. Simulation Setup

The widely known CST (Computer Simulation Technology) Microwave Studio Software was used to perform the simulations as well as the antenna design [12].

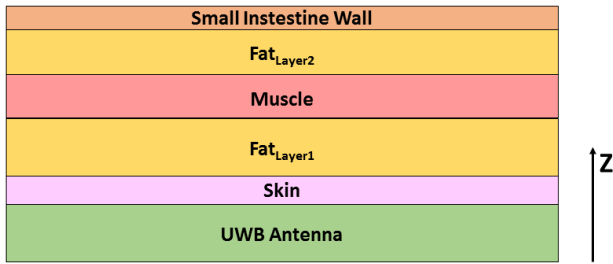


Fig. 1. Multilayer Antenna Model for the CST simulations.

In order to assess the antenna performance in a realistic environment, simulations considering the human body as a multilayer tissue model [5] were performed with CST. In particular, the multilayer model depicted in Fig. 1 was considered. The antenna was placed over five different tissue layers. These layers correspond with the main human body tissues involved in the transmission from the small intestine to the body surface as proposed in [11]. The antenna was considered to be in physical contact with the skin. The thickness of the skin layer was 1.5 mm. Two fat layers were taken into account. The thickness of  $Fat_{layer1}$  and  $Fat_{layer2}$  was 20 mm and 15 mm, respectively. Moreover, a muscle layer with thickness of 10 mm was placed between the fat layers aforementioned. The furthest tissue from the on-body antenna was a small intestine layer with thickness of 0.5 mm. The dielectric properties of human body tissues, electric conductivity and relative permittivity, were provided by C. Gabriel [2]. These values are based on Cole-Cole model, which describes the frequency dependence of the dielectric properties. From the Gabriel's data the dielectric features of human muscle tissue within UWB frequency range were entered in the CST in order to perform the simulations.

### B. Antenna Model

UWB On-body antennas for in-body communications should comply specific requirements. On the one hand, a compact structure is essential for wearable devices. On the other hand, a large bandwidth within UWB and good wave propagation conditions through the human tissues are needed. Slotted patch antenna models stand out for its main benefits at high frequencies such as its large bandwidth and

the high versatility of its designs [13]. Hence, this type of antennas might be an attractive candidate for this purpose. Accordingly, two UWB on-body slotted patch antennas have been designed, miniaturized and optimized considering the requirements mentioned above.

Regarding the antenna design, a fork-shaped microstrip feeding line structure was chosen. This is by the fact that this kind of feeding can get larger bandwidth than that obtained with a conventional feeding [14]. Using this feeding technique a really compact antenna structure can be achieved. In Fig. 2, the proposed feeding structure is shown.

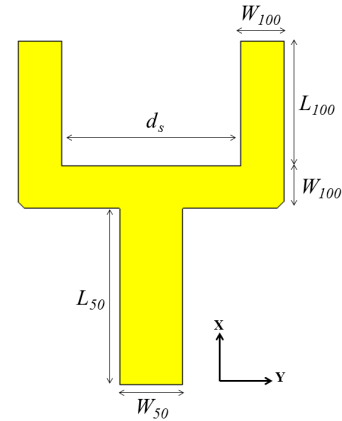


Fig. 2. Fork-shaped microstrip feeding line.

The fork-shaped structure is based on two symmetrical 100  $\Omega$  microstrip lines which are connected in parallel to the 50  $\Omega$  feed line. The microstrip feeding line width ( $W_{50} = 6.38$  mm), the stubs width ( $W_{100} = 4.30$  mm), and the separation between the two stubs ( $d_s = 18.13$  mm), were computed in order to achieve an input impedance of 50  $\Omega$ . Otherwise, the microstrip length was  $L_{50} = 12.67$  mm and the stubs length was  $L_{100} = 17.90$  mm.

The first design consisted in a conventional rectangular-shaped slotted patch in free space. The antenna structure was miniaturized and optimized by considering the five-layered model described in section II.A. In order to improve the bandwidth of this first antenna design, an enhanced stub loaded slotted patch antenna was carefully designed. This second design included two circles at the ends of the slot, for enhancing the impedance matching in a wider range of frequencies. These two designs are depicted in Fig. 3.

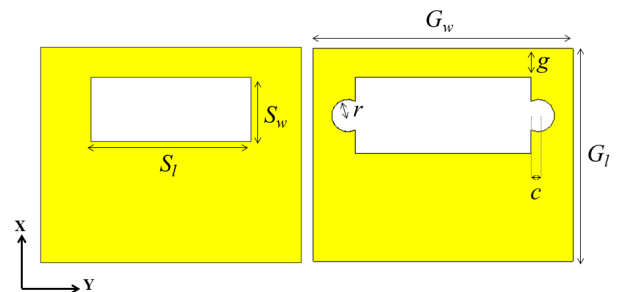


Fig. 3. Proposed slotted patch structures.

The ground plane dimensions were  $G_l = 40.5$  mm and  $G_w = 49.5$  mm. The rectangular slot width was  $S_w = 9.73$  mm and  $S_l = 23.56$  mm. The loaded slot with circles had a width of  $S_w = 14.55$  mm and a length of  $S_l = 33.5$  mm. The distance between the edge of the slot and the centre of the circle was  $c = 1.41$  mm, and the radius of the circle was  $r = 3$  mm. Finally, the gap between the slot and the upper edge of the ground plane was  $g = 5.50$  mm.

In order to receive the maximum power from sensors located inside the human body, it is important to focus the radiation pattern of the designed antenna in the direction of interest. Considering the slot antenna theory, this kind of structures presents omnidirectional radiation pattern [13]. To increase the directivity of the antenna while reducing the backward radiation, a reflecting element is included. Fig. 4 depicts the complete antenna structure including a reflecting plane and the dielectric substrate. On the one hand, the position and the size of the reflector were thoroughly studied in order to focus the power radiation in the desired direction. After an optimization process, a reflector length of  $R_l = 50$  mm, and a distance between the feeding structure and the reflector of  $d_r = 10$  mm, were chosen for this purpose. The width of the reflector,  $R_w$ , is equal to that of the ground plane ( $G_w$ ) in order to minimize the overall size of the antenna. Moreover, a Rogers 3003 dielectric substrate, which has a relative permittivity of 3 and a thickness of 1.524 mm, was used.

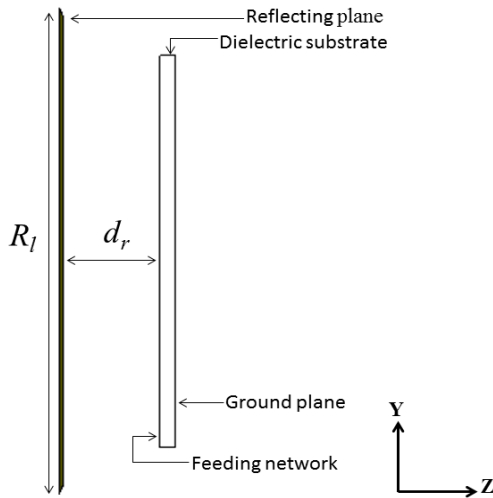


Fig. 4. Side view of the proposed antenna structure.

### III. RESULTS

#### A. Antenna Matching

Fig. 5 presents the simulated  $S_{11}$  for the slotted patch structures shown in Fig.3.

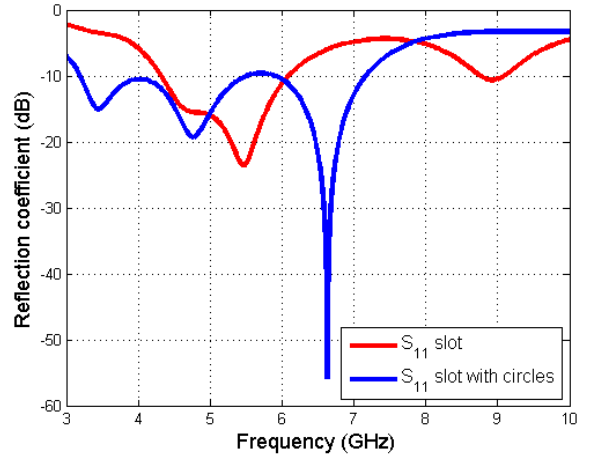
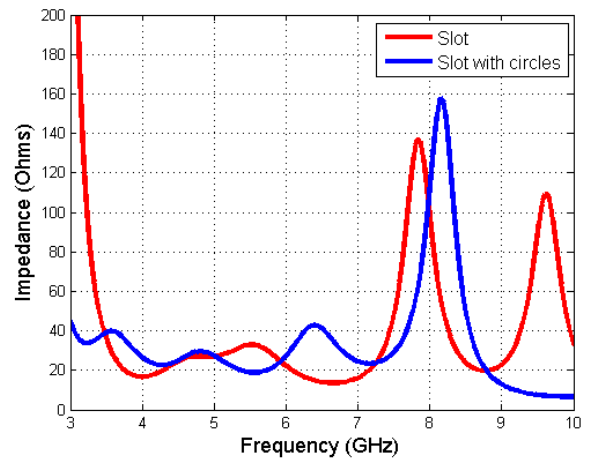


Fig. 5. Simulated  $S_{11}$  for the slotted patch structures of Fig.3 within UWB frequency band.

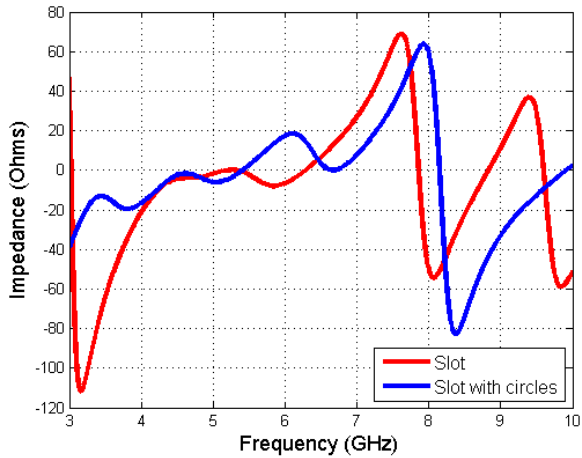
As can be observed in Fig. 5, the reflection coefficient obtained with the rectangular slot are below  $-10$  dB from 4.31 GHz to 6.10 GHz, which means an absolute bandwidth of 1.79 GHz and a relative bandwidth of 34.39 %. Moreover, it can be noted how the bandwidth improves by adding the circles at the ends of the slot. In this case, the antenna matching covers from 3.18 GHz to 5.52 GHz, achieving an absolute bandwidth of 2.34 GHz at the low part of UWB, and a relative bandwidth of 53.79 %. Besides, a matching band is achieved from 5.9 GHz to 7.15 GHz, obtaining an absolute bandwidth of 1.25 GHz and a relative bandwidth of 18.80 %. Thus, the optimization of the shape of the slot by adding the circles implies an improvement of the bandwidth of 550 MHz and 19.40 % in absolute and relative terms, respectively. Furthermore, an antenna matching within the low part of UWB frequency band is obtained.

#### B. Input Impedance

The real part of the input impedance of these two antennas is depicted in Fig. 6(a).



(a)



(b)

Fig. 6. Real (a) and imaginary (b) parts of complex impedance for each slot patch structure.

As can be seen from Fig. 6(a), the value of the resistance is stabilized between  $20 \Omega$  and  $50 \Omega$  from 3.1 GHz to 7.75 GHz in both designs. Moreover, as can be observed in Fig. 6(b), the reactance of the slot with circles is close to zero until 7.75 GHz. On the contrary, in the case of the rectangular slot, the reactance is close to zero in a narrow frequency band. This fact implies the larger bandwidth obtained with the slot loaded with circles.

### C. Near-field Radiation pattern

Considering the antenna dimensions, the wavelength in the frequency band of interest, and the tissues permittivity and thickness, it can be concluded that the antenna radiation range is on the Fresnel region [15]. For this reason, near-field radiation pattern of the slot loaded with circles is studied.

Fig. 7 shows the near-field radiation patterns of the slot with circles from 3.1 GHz to 6.1 GHz.

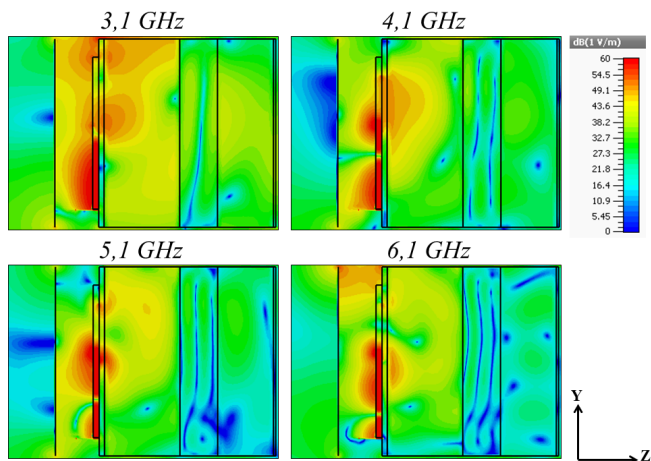


Fig. 7. Near radiated E-Field (dBV/m) in the human tissues.

As can be seen, the slot loaded with circles achieves good results in terms of field penetration into the human tissues. However, as expected, both field penetration and near-field radiating pattern get worse as the frequency increases. This happens because the losses in the human tissues grow as the frequency increases [2]. On the other hand, the effect of the reflecting plane can be noted. The electrical field is focused into the human tissues and the penetration through them increases. Moreover, the backward radiation is minimized as expected.

### D. Testing

A prototype of the slot loaded with circles was fabricated at our facilities. In Fig. 8, the manufactured model of this design is shown. In order to hold the reflector plane and increase the consistency of the whole structure, four nylon screws were included during the manufacturing process.

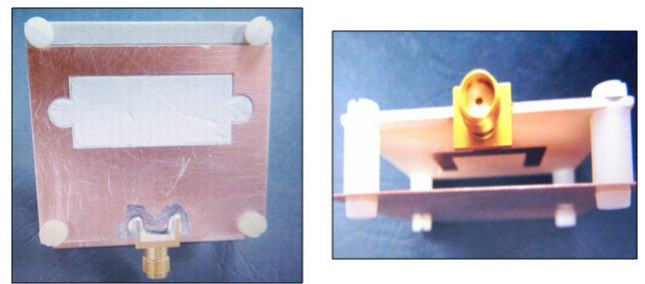


Fig. 8. Manufactured prototype of the slot loaded with circles patch antenna designed.

After the manufacturing process, the antenna performance was checked in order to verify the accuracy of the simulation setup considered in the design stage. Hence,  $S_{11}$  was measured with the antenna placed on the human belly. In Fig. 9, the measurement setup is shown. In order to measure the reflection coefficient, a Keysight N5227A vector network analyzer (VNA) was used. The VNA was calibrated through a full port calibration within the entire frequency band (2 - 11 GHz). To protect the antenna, and avoid direct contact with the skin, it was covered with a plastic bag in the measurement process.

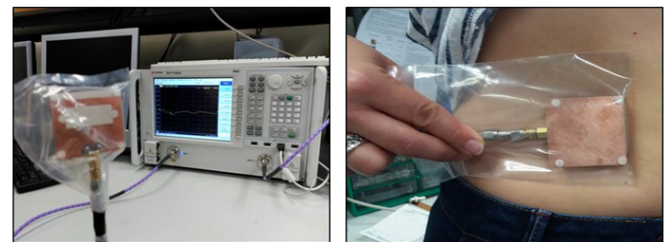


Fig. 9. Measurement setup.

Fig. 10 compares the measured and simulated  $S_{11}$  of the slot patch antenna loaded with circles. It can be observed that both results are in close agreement. The slight differences observed can be attributed to the divergences

between the thickness of the tissue layers of the human subject used during the measurements and the thickness of the tissues used in the simulation process, along with the use of the plastic bag. Nevertheless,  $S_{11}$  values are still below -6 dB between 3 GHz and 5.3 GHz, achieving an absolute bandwidth greater than 2 GHz within the low part of UWB in a harsh communications scenario as the human body is.

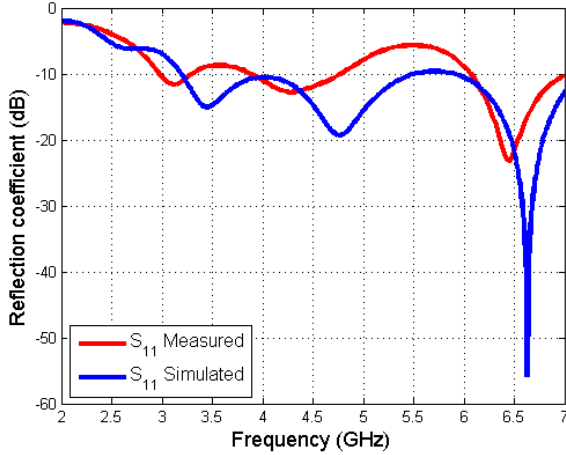


Fig. 10. Simulated and measured  $S_{11}$ .

#### IV. CONCLUSIONS

In this work, several UWB on-body slotted patch antenna models for in-body communications are studied. These antennas were designed to establish a proper link with an implanted device located inside the human small intestine. The shape and size of the antennas were first optimized with CST software in a realistic in-body scenario modeling the human tissues as layers of proper permittivity. Before manufacturing a definitive antenna prototype, several antenna models were tested. Finally, an optimized antenna model was chosen, and a first prototype was fabricated in our facilities. In order to assess the performance of the manufactured antenna and the reliability of the simulation setup, the  $S_{11}$  was measured when the antenna was placed on the human belly.

As evidenced by the results, the optimized slotted patch antenna loaded with circles achieves a bandwidth larger than 2 GHz in the low part of UWB frequency band. Furthermore, the slot patch antenna loaded with circles has good field penetration through the human tissues. The reflection coefficient measured within UWB, when the proposed antenna was placed in the human belly, was in good agreement with simulated results, so the reliability of our simulation setup was confirmed.

Since the thickness of each human tissue is different according to the assessed human subject, our new antenna should be tested in more ex vivo experiments. Besides, the UWB channel performance using on-body slot patch antennas and an implanted antenna should be studied.

#### REFERENCES

- [1] R. Chavez-Santiago and I. Balasingham, "Ultrawideband Signals in Medicine," *IEEE Signal Process. Mag.*, vol. 31, no. 6, pp. 130–136, Nov. 2014.
- [2] C. Gabriel, "Compilation of the Dielectric Properties of Body Tissues at RF and Microwave Frequencies." Brooks Air Force, N.AL/OE-TR- 1996-0037, San Antonio, TX, 1996.
- [3] R. Chávez-Santiago *et al.*, "Propagation models for IEEE 802.15.6 standardization of implant communication in body area networks," *IEEE Commun. Mag.*, vol. 51, no. 8, pp. 80–87, Aug. 2013.
- [4] A. Khaleghi, R. Chávez-Santiago, and I. Balasingham, "Ultrawideband statistical propagation channel model for implant sensors in the human chest," *IET Microwaves, Antennas Propag.*, vol. 5, no. 15, p. 1805, 2011.
- [5] E. Pancera, Xuyang Li, M. Jalilvand, T. Zwick, and W. Wiesbeck, "UWB medical diagnostic: in-body transmission modeling and applications." pp. 2651–2655, 2011.
- [6] L. A. Yimjjo Poffelie, P. J. Soh, S. Yan, and G. A. E. Vandenbosch, "A High-Fidelity All-Textile UWB Antenna With Low Back Radiation for Off-Body WBAN Applications," *IEEE Trans. Antennas Propag.*, vol. 64, no. 2, pp. 757–760, Feb. 2016.
- [7] S. Kang and C. W. Jung, "Wearable fabric reconfigurable beam steering antenna for on/off-body communication system," in *IEEE International Symposium on Antennas and Propagation & USNC/URSI National Radio Science Meeting*, 2015, pp. 1211–1212.
- [8] W. Jeong and J. Choi, "A low profile IR-UWB antenna with conical radiation pattern for on-body communications," in *IEEE International Symposium on Antennas and Propagation & USNC/URSI National Radio Science Meeting*, 2015, pp. 2023–2024.
- [9] M. Klemm, I. Z. Kovcs, G. F. Pedersen, and G. Troster, "Novel small-size directional antenna for UWB WBAN/WPAN applications," *IEEE Trans. Antennas Propag.*, vol. 53, no. 12, pp. 3884–3896, Dec. 2005.
- [10] Xianming Qing, M. Y. W. Chia, and Xuanhui Wu, "Wide-slot antenna for UWB applications," in *IEEE Antennas and Propagation Society International Symposium. Digest. Held in conjunction with: USNC/CNC/URSI North American Radio Sci. Meeting (Cat. No.03CH37450)*, vol. 1, pp. 834–837.
- [11] P. Ara, M. Heimlich, and E. Dutkiewicz, "Antenna performance for localization of capsule endoscope," in *8th International Symposium on Medical Information and Communication Technology (ISMICT)*, 2014, pp. 1–5.
- [12] T. Weiland, M. Timm, and I. Munteanu, "A practical guide to 3-D simulation," *IEEE Microw. Mag.*, vol. 9, no. 6, pp. 62–75, Dec. 2008.
- [13] C. A. Balanis, *Antenna Theory: Analysis and Design*, 3rd ed. John Wiley & Sons, 2005.
- [14] S. D. Targonski, R. B. Waterhouse, and D. M. Pozar, "Design of wide-band aperture-stacked patch microstrip antennas," *IEEE Trans. Antennas Propag.*, vol. 46, no. 9, pp. 1245–1251, 1998.
- [15] P. S. Hall and Y. Hao, "Antennas and propagation for body-centric wireless communications," 2006, p. 258.